THE JOURNAL OF PHYSICAL CHEMISTRY B

ARTICLE

pubs.acs.org/JPCB

Factors Affecting the Size and Uniformity of Hollow Poly(lactic acid) Microcapsules Fabricated from Microbubble Templates

Jay Jesus Molino Cornejo,[†] Hirofumi Daiguji,*[,†] and Fumio Takemura[‡]

[†]Division of Environmental Studies, Graduate School of Frontier Sciences, The University of Tokyo, 5-1-5 Kashiwanoha, Kashiwa 277-8563, Japan

[‡]National Institute of Advanced Industrial Science and Technology (AIST), 1-2-1 Namiki, Tsukuba 305-8564, Japan

Supporting Information

ABSTRACT: Hollow microcapsules of poly(lactic acid) (PLA) were fabricated using the bubble template method, which involves the nucleation of bubbles inside droplets of a dichloromethane solution of PLA prepared in a continuum medium of an aqueous solution of poly(vinyl alcohol) (PVA). PLA-covered microbubbles are formed by PLA adsorbing onto the microbubble surface and then spontaneously released from the dichloromethane droplets into the surrounding aqueous solution. Thereby, hollow PLA microcapsules are formed. In the present study, we focus on the effects of the initial PLA concentration, addition of PVA to the aqueous medium, and PLA molecular weight on the radius distribution of the hollow PLA microcapsules. Results show that a low initial concentration of PLA, the addition of PVA, and low molecular weight PLA are required to form uniform hollow microcapsules. It is suggested that these factors reduce the energy barrier at the liquid−liquid interface, which allows the PLA-covered microbubbles to pass smoothly through the interface. Furthermore, we observed the release of the microbubbles from the dichloromethane droplets through a microscope and clarified the relationship between the uniformity of the hollow PLA microcapsules and the bubble-release mechanism.

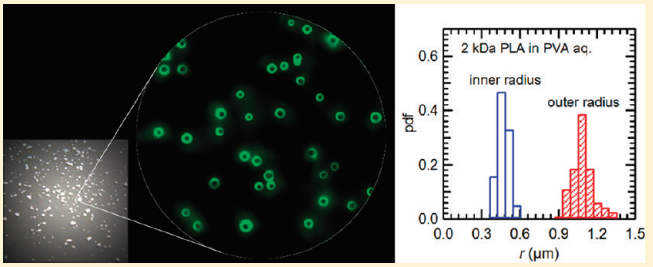

1. INTRODUCTION

Ultrasound is the most versatile, noninvasive, low-cost, and low-risk real-time imaging technique to visualize the condition of internal tissues. However, despite its widespread application, the capabilities of this method are hindered by a lack of effective ultrasound contrast agents.[1,2] Contrast agents are used to alter the image contrast to improve the diagnostic yield, thereby enabling physicians to easily and clearly distinguish between normal and abnormal conditions.[3]

Microbubbles can potentially be used as echo enhancers.[4−7] Since the acoustic impedance between blood and gas in a bubble is high, incident waves are completely reflected. However, if microbubbles are to be used as standalone ultrasound contrast agents, several issues must be addressed. They have a short lifespan in the system, which is further shortened in the presence of an ultrasound field.[1,8] Also, they rapidly disappear in the blood after they are infused intravenously.[8−11] Even if they are stabilized with lipid bilayers, the microbubbles rapidly disintegrate because the interactions between lipid molecules are weak.[12] In addition, microbubbles must be in the size range of 1−4 μm to easily pass through the capillary blood circuit and ensure a long circulation time before they completely drain into the liver.[1,13] However, it is difficult to control the size of microbubbles. Furthermore, because the resonant frequency of a microbubble is a function of its radius, it is vital for microbubbles to be uniformly sized in order to attain a narrow backscatter signal.

It is desirable to have highly uniform functionalized microbubbles with an increased lifespan within the optimum size range for ultrasound applications. Therefore, if microbubbles could be conveniently wrapped in a biodegradable polymer, they could be effectively employed as ultrasound contrast agents. The shell must be solid to eliminate surface tension and decrease gas permeability through the shell, but it should also be sufficiently thin and flexible to allow the bubble to resonate.

In this study, we focused on hollow microcapsules intended for use as ultrasound contrast agents. A hollow microcapsule is a microbubble encapsulated by a polymer shell; it can also be described as a gas-filled (e.g., CO_2, N_2, perfluorocarbons, etc.) spherical particle.[5,6,14] To synthesize hollow microcapsules, current manufacturing techniques rely on the use of sacrificial liquid or solid cores onto which the biodegradable polymeric layer can be formed via polymerization or adsorption. After the formation of the capsule shell, the strength of the shell is intentionally degraded by aging or cross-linking so that the liquid or solid core can be removed by dissolution, evaporation, or

Received: August 21, 2011
Revised: October 7, 2011
Published: October 20, 2011

thermolysis to yield hollow microcapsules. Therefore, the complexity of these synthetic procedures is reduced if a gas core is used as the microcapsule template.[15]

In our previous studies, we successfully demonstrated the fabrication of hollow PLA microcapsules using the bubble template method[16] and identified the two sets of conditions required for this method: (1) the conditions required for maintaining the stability of the uniformly sized microbubbles inside a droplet of a dichloromethane solution of PLA, and (2) the conditions required for the release of hollow PLA microcapsules from the droplet.[17] However, it remains a challenge to control the size and uniformity of the hollow PLA microcapsules because they are sensitive to the various fabrication conditions. Furthermore, although the mean radius of the template microbubbles agreed with the theoretical prediction,[18] the mean inner capsule radius was smaller than the original microbubble template. These results imply that the hollow PLA microcapsules shrank before the shell solidified. To more precisely control the size of these hollow PLA microcapsules, the fabrication conditions, influence of the chemical composition, and bubble-release mechanism must be elucidated.

In this study, we focused on the effects of the initial PLA concentration, addition of PVA to the aqueous medium, and PLA molecular weight on the radius distribution of the fabricated hollow PLA microcapsules. Furthermore, we discuss the bubble-release mechanism to enable more precise size control of the hollow PLA microcapsules.

2. EXPERIMENTAL METHODS

2.1. Chemicals. The polymeric shell material comprised PLA with molecular weights of 2, 45, and 100 kDa (PolyScience, Niles, IL), dichloromethane of 99.99% purity (Wako, Osaka, Japan), and aqueous phase 2% (w/w) PVA (Gohsenal T-350, Nippon Gohsei, Osaka, Japan). All the chemicals used in this study were reagent grade. Water from a Milli-Q Advantage A10 water purification system was used.

2.2. Method. The synthesis method of hollow PLA microcapsules was as follows: 1 mm radius droplets of a dichloromethane solution of PLA were formed and dispersed gently in a continuous phase made of either a 2% (w/w) PVA aqueous solution or pure water through a microsyringe. In the PVA aqueous solution, even if the droplets got into contact, they did not coalesce due to the surface-active properties of PVA, whereas in water, special care was taken during the droplet formation process to avoid coalescence. Immediately after formation, diffusion of dichloromethane into the continuous phase took place, allowing microbubble nucleation to start. Subsequently, PLA adsorbed on the microbubble surface yielding to microcapsules that were spontaneously released from the droplet into the continuous phase. The generated hollow PLA microcapsules were collected and purified. This process involves several filtering stages and abundant water to ensure the complete removal of any PVA film that might have surrounded the capsule shell. The hollow PLA microcapsules were dried for 36 h using silica gel. Finally, the hollow PLA microcapsules were obtained as a white powder. The shells of the obtained hollow PLA microcapsules were sufficiently solid to retain their forms in the dry condition. Prior to synthesis, the PLA was stained with Nile red to obtain the fluorescent images.

Attempts were made to control the capsule size distribution by changing the following three parameters: (1) the initial PLA concentration of the dichloromethane solution, (2) the concentration of PVA in the aqueous medium, and (3) the PLA molecular weight. To assess the effect of each parameter on the final capsule size, several bright-field and fluorescent images of the dried hollow PLA microcapsules were obtained using an inverted microscope (ECLIPSE Ti-E, Nikon Corp., Tokyo, Japan). Dried capsules were placed on a glass bottom dish. We employed a 60× water immersion objective lens that has a depth of field of 0.4 μm. Thus, due to the size range of the analyzed microcapsules, it was plausible to say that all the microcapsules in the snapshots were in focus. Furthermore, when the microscope was used in fluorescent mode, since only the capsule shell was stained with fluorescein, the existence of a gas inner core could be confirmed as there was no fluorescence coming from it.

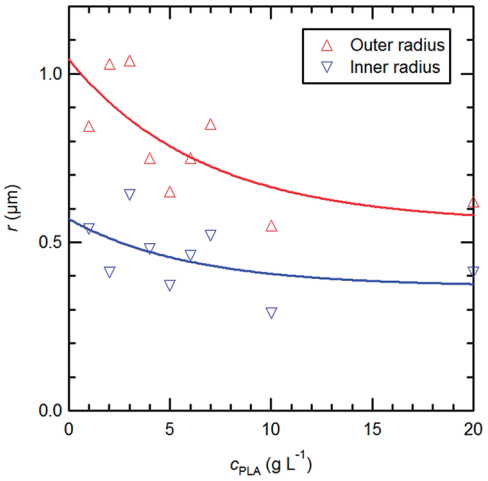

Figure 1. Mean inner and outer radii of hollow PLA microcapsules fabricated in a 2% (w/w) PVA aqueous solution as a function of the initial PLA concentration.

To determine the effect of the initial PLA concentration, 1, 2, 3, 4, 5, 6, 7, 10, and 20 g L^{-1} dichloromethane solutions of 2 kDa PLA were prepared. To clarify the effect of the addition of PVA, we used both pure water and a 2% (w/w) PVA aqueous solution as the surrounding aqueous medium. The initial PLA concentration was 2 g L^{-1} and 2 kDa PLA was employed in this experiment. Additionally, dichloromethane solutions of 2, 45, and 100 kDa PLA were prepared to assess the effect of the molecular weight of PLA. In this experiment, the initial concentration of PLA was set at 2 g L^{-1} and hollow PLA microcapsules were fabricated both in a 2% (w/w) PVA aqueous solution and in pure water. All experiments were performed at room temperature and atmospheric pressure.

3. RESULTS

3.1. Effect of Initial PLA Concentration. In our previous study,[17] the effect of the initial PLA concentration was investigated to determine the conditions required for the release of the PLA-covered microbubbles from the droplets. The results showed that the release of the bubbles began when the PLA concentration of the dichloromethane solution exceeded 5 g L^{-1} regardless of the initial concentration. However, the sizes of the fabricated hollow PLA microcapsules were not evaluated. In the present study, the initial concentration of 2 kDa PLA in dichloromethane was varied to analyze its effect on the final microcapsule size. Figure 1 shows the mean inner and outer radii

Table 1. Measured Capsule Radius As a Function of the Initial PLA Concentration[a]

PLA concn (g L^{-1})	radius	mean radius (μm)	std dev (μm)	PI (%)
1	outer	0.84	0.24	28.6
	inner	0.54	0.20	37.0
2	outer	1.03	0.07	7.7
	inner	0.41	0.04	10.3
3	outer	1.04	0.06	5.8
	inner	0.64	0.08	12.5
4	outer	0.75	0.16	21.6
	inner	0.48	0.15	32.1
5	outer	0.65	0.14	21.5
	inner	0.37	0.12	32.4
6	outer	0.75	0.23	30.6
	inner	0.46	0.15	32.6
7	outer	0.85	0.21	24.7
	inner	0.52	0.16	30.8
10	outer	0.55	0.21	38.2
	inner	0.29	0.13	44.8
20	outer	0.62	0.24	38.7
	inner	0.41	0.20	48.8

[a] The molecular weight of PLA was 2 kDa and the aqueous medium was a 2% (w/w) PVA aqueous solution.

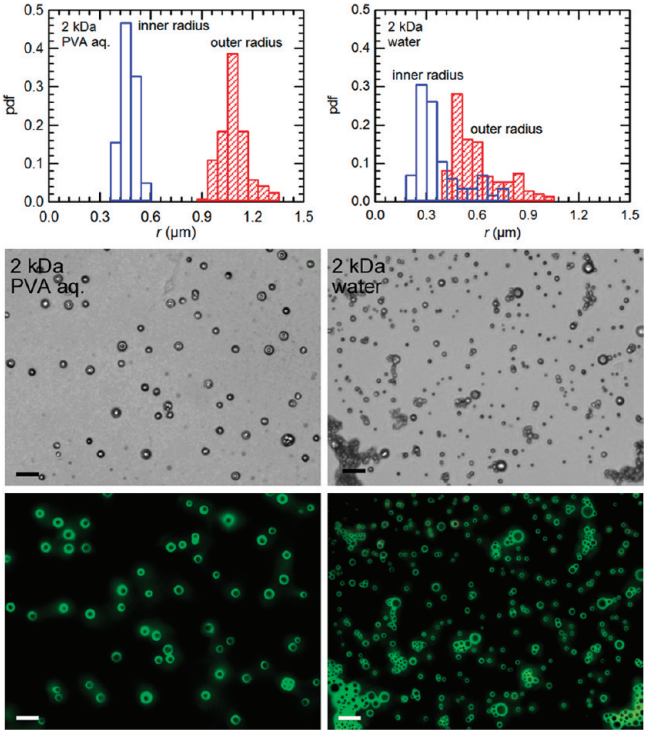

Figure 2. Probability density function (PDF) (top) and typical bright field (middle) and fluorescent (bottom) images of the hollow PLA microcapsules fabricated in a 2% (w/w) PVA aqueous solution (left) and water (right). The initial PLA concentration was 2 g L^{-1} and the PLA molecular weight was 2 kDa. The scale bar is 5 μm long.

of the hollow PLA microcapsules fabricated in the 2% (w/w) PVA aqueous solution. Although the data were scattered, it was

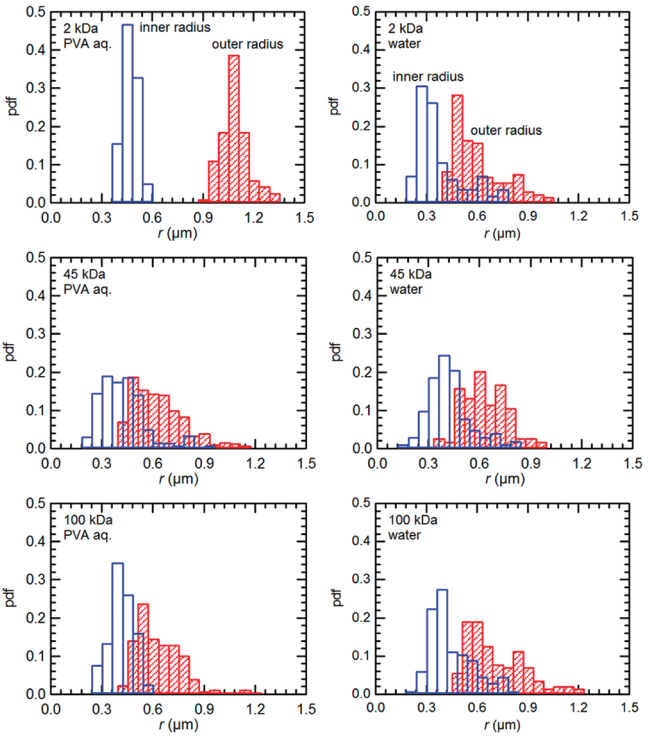

Figure 3. Probability density function (PDF) of hollow PLA microcapsules of different molecular weights, i.e., 2 kDa (top), 45 kDa (middle), and 100 kDa (bottom), fabricated in a 2% (w/w) PVA aqueous solution (left) and water (right). The initial PLA concentration was 2 g L^{-1}.

found that the outer and inner radii decreased with an increase in the initial PLA concentration. The thickness of the microcapsule shell also decreased with an increase in the initial PLA concentration. The mean values, standard deviations, and polydispersity indices (PI = standard deviation/mean) of the outer and inner radii are summarized in Table 1. The PI values of the outer and inner radii were around 10% when the initial PLA concentration was either 2 or 3 g L^{-1}, which suggests that hollow PLA microcapsules fabricated under these conditions were highly uniform.

These results suggest that the initial PLA concentration should be much less than 5 g L^{-1} to delay the release of the bubbles until the dissolved PLA molecules adsorb on the nucleated bubble surface. When the initial PLA concentration was too high, the dissolved PLA molecules adsorbed on the interface between the droplet and the surrounding aqueous medium, thus preventing the bubbles from passing smoothly through the interface. On the other hand, when the initial PLA concentration was too low, the PI value increased, which suggests that the bubbles were not effectively covered with PLA.

3.2. Effect of PVA. Figure 2 shows the probability density function and typical bright-field and fluorescent images of hollow PLA microcapsules fabricated in either a 2% (w/w) PVA aqueous solution or water. The initial PLA concentration was 2 g L^{-1} and the PLA molecular weight was 2 kDa. The inner and outer radii of the hollow PLA microcapsules fabricated in water were smaller than those fabricated in the 2% (w/w) PVA aqueous solution. In addition, the standard deviation of the radii of the microcapsules was larger when they were fabricated in water rather than in the 2% (w/w) PVA aqueous solution.

Table 2. Measured Inner and Outer Radii of the Hollow PLA Microcapsules[a]

MW of PLA and type of aq medium	radius	mean (μm)	std dev (μm)	PI (%)
2 kDa in 2% (w/w) PVA aq	outer	1.03	0.08	7.7
	inner	0.41	0.04	10.3
45 kDa in 2% (w/w) PVA aq	outer	0.58	0.15	26.7
	inner	0.36	0.13	37.8
100 kDa in 2% (w/w) PVA aq	outer	0.58	0.14	25.0
	inner	0.36	0.07	20.1
2 kDa in water	outer	0.55	0.15	27.5
	inner	0.32	0.14	43.3
45 kDa in water	outer	0.57	0.13	23.2
	inner	0.37	0.13	34.7
100 kDa in water	outer	0.65	0.17	26.0
	inner	0.39	0.13	33.4

[a] The initial PLA concentration of the dichloromethane solution was 2 g L^{-1}.

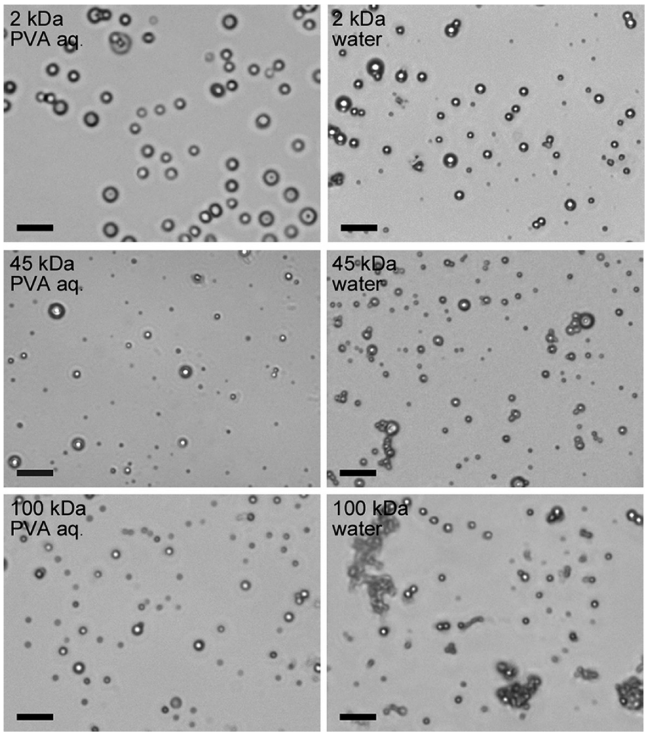

Figure 4. Typical bright field images of hollow PLA microcapsules of different molecular weights, i.e., 2 kDa (top), 45 kDa (middle), and 100 kDa (bottom), fabricated in a 2% (w/w) PVA aqueous solution (left) and water (right). The initial PLA concentration was 2 g L^{-1}. The scale bar is 5 μm long.

In our previous study,[16,17] we used a 2% (w/w) PVA aqueous solution as a continuum medium to prevent the droplets of dichloromethane from coalescing due to the surface active properties of PVA on the droplet surface. Figure 2 shows that hollow PLA microcapsules can be formed in both the 2% (w/w) PVA aqueous solution and water; thus, the addition of PVA is not required to form the microcapsules, although it does affect the capsule size distribution.

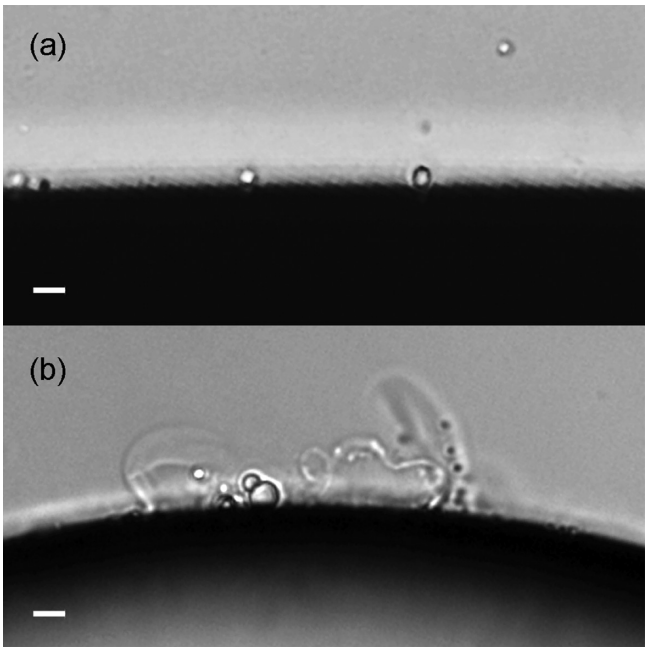

Figure 5. Two release mechanisms of microbubbles: (a) single-bubble release as a result of solvent evaporation and (b) multiple-bubble release as a result of bubble eruption. The initial PLA concentrations of the dichloromethane solutions are (a) 2 and (b) 20 g L^{-1}. The PLA molecular weight was 2 kDa and the surrounding aqueous medium was 2% (w/w) PVA aqueous solution in both cases. The scale bar is 10 μm long.

3.3. Effect of PLA Molecular Weight. Figure 3 shows the probability density function for the hollow PLA microcapsules manufactured using three different molecular weights of PLA (i.e., 2, 45, and 100 kDa) fabricated in either a 2% (w/w) PVA aqueous solution or water. The initial PLA concentration was 2 g L^{-1}. The measured inner and outer radii of these hollow PLA microcapsules are summarized in Table 2. Figure 4 shows the corresponding typical bright-field images. In the 2% (w/w) PVA aqueous solution, the outer radius and shell thickness of the hollow PLA microcapsules decreased and the uniformity deteriorated as the molecular weight increased. PLA microparticles in addition to hollow PLA microcapsules were produced at molecular weights of 45 and 100 kDa. However, the fabricated microcapsules showed high PI values regardless of the molecular weight. It was observed that the number of PLA microparticles and aggregates of hollow PLA microcapsules increased with increased molecular weight.

These results indicate that the addition of PVA and low molecular weight PLA yielded large and highly uniform hollow PLA microcapsules. Among the six conditions shown in Figures 3 and 4, the uniformity of the hollow PLA microcapsules was only very high when the PLA molecular weight was 2 kDa and the aqueous medium was the 2% (w/w) PVA aqueous solution. Additionally, using these conditions very few microparticles and aggregates of hollow microcapsules were observed. This indicates that the mechanism of capsule shell formation depends on the PLA molecular weight as well as the addition of PVA.

4. DISCUSSION

4.1. Observation of Microbubble Release from the Dichloromethane Droplet. In the bubble-template method, the

Table 3. Measured Interfacial Tensions between the Liquid−Liquid Interfaces at 298 K

liquid−liquid interface	interfacial tension (N m^{-1})
dichloromethane−water	0.0281
dichloromethane−2% (w/w) PVA aqueous solution	0.0194
2 g L^{-1} PLA (2 kDa) dichloromethane solution−water	0.0269
2 g L^{-1} PLA (2 kDa) dichloromethane solution−2% (w/w) PVA aqueous solution	0.0189

size and uniformity of the fabricated PLA microcapsules should correlate with the bubble-release mechanism. First, the release of the microbubbles from the dichloromethane droplets was observed through a microscope; two typical snapshots are shown in Figure 5. As shown in Figure 5a, each microbubble independently appeared on the droplet surface, detached from the surface, and moving into the aqueous medium. In this mechanism, it appears that the PLA-covered microbubbles are gradually exposed to the surrounding aqueous medium as solvent evaporation occurs. This mechanism was observed under most experimental conditions. However, the PLA-covered microbubbles are smoothly released from the interior with a low initial concentration of PLA, the addition of PVA, and a low molecular weight of PLA. Except for under these experimental conditions, as dichloromethane diffuses from the droplet into the surrounding aqueous medium the droplet shrinks and a high-PLA-concentration region grows at the liquid−liquid interface. Thus, when the microbubbles reach the interface, they stay there. Since the bubbles keep nucleating as a result of solvent diffusion, more and more bubbles aggregate. Under these conditions, the release of microbubbles shown in Figure 5b was observed. The shadow in the aqueous medium reflects the differences in density; that is, dichloromethane flow from the droplet is accompanied with microbubble emission. From these two images, the bubble-release mechanism can be classified as either single-bubble release due to solvent evaporation (Figure 5a) or multiple-bubble release as a result of bubble eruption (Figure 5b). The first mechanism is required for the fabrication of uniformly sized hollow PLA microcapsules.

The bubble-release mechanism seems to depend on the energy barrier at the liquid−liquid interface. The low energy barrier at the liquid−liquid interface allows a single PLA-coated microbubble to pass smoothly through the interface. The suitable conditions for single bubble release: a low initial concentration of PLA, the addition of PVA, and a low molecular weight of PLA can reduce the energy barrier at the liquid−liquid interface. In the following section, the energy barrier at the liquid−liquid interface and single bubble-release mechanism to break the energy barrier were discussed.

4.2. Single Bubble Release Mechanism. To quantitatively discuss the single bubble release mechanism, the interfacial tension, droplet reduction rate, and viscosity were measured. The interfacial tensions were measured by the pendant drop method using the Drop Master Series DM-501 (Kyowa Interface Science, Japan) (see Supporting Information, Figure S1) and are summarized in Table 3. The measured interfacial tensions between dichloromethane−water and dichloromethane−2% (w/w) PVA aqueous solution were 2.81×10^{-2} and 1.94×10^{-2} N m^{-1}, respectively, at 298 K. This result suggests that PVA adsorbed on the interface between the droplet and the surrounding aqueous medium, resulting in decreased the interfacial tension.[19] If a 2 g L^{-1} PLA (2 kDa) dichloromethane solution was employed instead of pure dichloromethane, the measured interfacial tensions slightly decreased, as shown in Table 3. Although the effect of PLA on the interfacial tension was small, the PLA reduced the diffusivity of dichloromethane into the surrounding aqueous medium, which was confirmed by the difference of the size reduction rate of the droplets (see Supporting Information, Figure S2). Therefore, the addition of PLA creates a more stable liquid−liquid interface. Furthermore, the viscosity of polymer solutions generally increases with increasing polymer concentration and polymer molecular weight.[20] We confirmed that the viscosity of the PLA dichloromethane solutions increased with increasing PLA concentration and PLA molecular weight by measuring the viscosity of the solutions using a tuning fork vibration viscometer (SV-10, A&D Co., Japan). The measured viscosity of dichloromethane was 0.43×10^{-3} Pa s at 298 K. Upon the addition of 2 kDa PLA, the measured viscosities at 298 K were 0.47×10^{-3} and 1.07×10^{-3} Pa s for concentrations of 2 and 70 g L^{-1}, respectively (see Supporting Information, Figure S3).

To explain the bubble-release mechanism at the liquid−liquid interface, we must prove the following:

(1) a droplet has sufficient potential energy for continuous bubble release;
(2) a force sufficient to break the interfacial tension can be produced at or near the interface.

Assuming that a bubble is spherical with a radius of r_0, the energy required for a single bubble to pass through the interface is given by the following equation:

$$E_0 = \pi {r_0}^2 \gamma \tag{1}$$

where γ is the interfacial tension at the liquid−liquid interface. The potential energy of a droplet of a dichloromethane solution of PLA is equivalent to the energy of the buoyancy of the bubbles when the dissolved air is nucleated. Assuming that the droplet is spherical with a radius of r and bubbles initially nucleate at the center of the droplet and then elevate to the top of the droplet, the potential energy of a single bubble due to buoyancy is given by

$$E_1 = \rho g r \frac{4}{3} \pi {r_0}^3 \tag{2}$$

where ρ is the liquid density and g is gravitational acceleration. Since the volume ratio of dissolved air to dichloromethane is about 0.13,[21] the volume of dissolved air inside the droplet is $0.13 \times (4/3)\pi r^3$. If the droplet shrinks by n times, the total volume of the nucleated bubbles is $(1 - 1/n) \times 0.13 \times (4/3)\pi r^3$; thus, the total number of nucleated bubbles is

$$N = \left(1 - \frac{1}{n}\right) \times 0.13 \times \left(\frac{r}{r_0}\right)^3 \tag{3}$$

From eqs 2 and 3, the total potential energy of a droplet of dichloromethane solution of PLA is

$$E_N = NE_1 = \left(1 - \frac{1}{n}\right) \times 0.13 \times \frac{4}{3} \pi \rho g r^4 \tag{4}$$

Assuming that r_0 is 10^{-6} m, r is 5.0×10^{-4} m, γ is 2.0×10^{-2} N m^{-1}, ρ is 1.33×10^3 kg m^{-3}, and g is 9.8 m^2 s^{-1}, E_0 and E_N are calculated to be 6.28×10^{-14} J and $(1 - 1/n) \times 4.43 \times 10^{-10}$ J,

respectively. Thus, if $n = 2$, E_N is 3.5×10^3 times larger than E_0. Therefore, the potential energy of a droplet of dichloromethane solution of PLA is large enough for single-bubble release.

The average pressure inside a dichloromethane droplet should equilibrate with the pressure of the surrounding aqueous medium, but, for single-bubble release, the local and instantaneous pressure around a bubble must be larger than the equilibrium pressure. The required pressure difference is given by

$$\Delta p = \frac{2\gamma}{r_0} \tag{5}$$

Assuming that r_0 is 10^{-6} m, Δp was calculated to be 53.8 and 37.8 kPa for $\gamma = 2.69 \times 10^{-2}$ and 1.89×10^{-2} N m^{-1}, respectively. During the microscopic observations, a circulation flow, which had a maximum velocity in the order of 10^{-4} m s^{-1}, was generated inside the dichloromethane droplets due to the buoyancy of the nucleated bubbles. The Reynolds number for this flow can be estimated to be Re = u (velocity) $\times$ r_0 (bubble radius) $\times$ η (viscosity)$^{-1}$ $\times$ ρ (density) = 10^{-5} m s^{-1} $\times$ 10^{-6} m $\times$ $(10^{-3}$ Pa s$)^{-1}$ $\times$ 10^3 kg m^{-3} = 10^{-5}, which suggests that Stokes flow can be assumed. In fact, when single-bubble release occurred, no turbulence was observed. Assuming that the dichloromethane droplet is spherical and the dichloromethane flows up along the vertical axis and then down along the circumference from the top to the bottom of the sphere, if the flow in the circumferential direction constantly decelerates, pressure is generated in the radial direction. The pressure in the radial direction can be approximately estimated using the following Stokes equation:

$$\frac{dp_r}{dr} = -\eta \frac{2}{r^2} \frac{du_\theta}{d\theta} \tag{6}$$

where η is the viscosity of the solution, r is the radius of the droplet, θ is the inclination angle, and u_θ is the velocity in the inclination angle direction. We focus on the force balance in a small portion of the outermost spherical shell (i.e., dr, $r\,d\theta$, $r\,d\varphi$, where φ is azimuth angle). Assuming that η is 10^{-3} Pa s, r is 10^{-4} m, dr is 10^{-5} m, and $(du_\theta/r\,d\theta) = -(10^{-5}$ m s$^{-1}/10^{-5}$ m), dp_r is calculated to be 2×10^{-4} Pa, which is far smaller than the pressure difference required for single-bubble release. Even if the pressure in the radial directions integrated over the surface of the droplet is focused on a single bubble, the pressure affecting a single bubble is calculated to be 8 Pa ($dp_r \times (4\pi r^2/\pi r_0^2)$). The radial pressure created by deceleration of circular flow does not reach the required pressure difference. However, in a real system, many bubbles are distributed at the liquid−liquid interface. In such conditions, the bubbles interact with each other and the local and instantaneous pressure affecting each bubble may overcome the pressure required for single-bubble release. The repulsive force between two adjacent bubbles is generally quite large. Furthermore, the deformation of bubbles and the squeezing flow between bubbles may change the direction of a bubble with respect to the aqueous medium.[22] To clarify this release mechanism, it is necessary to make a model of the bubble dynamics at the liquid−liquid interface.

Another possible mechanism for single-bubble release is the imbalance of interfacial tensions around a bubble during the diffusion of dichloromethane into the surrounding aqueous medium. Figure 6 shows a schematic of the interfacial tensions at the triple phase interface between an aqueous phase (a), an organic phase (o), and a gas phase (g). The water−air, $\gamma_{w\text{-}air}$, and dichloromethane−air, $\gamma_{d\text{-}air}$, interfacial tensions are 7.18×10^{-2} and 2.72×10^{-2} N m^{-1}, respectively, at 298 K. However, in a real system, water containing PLA, dichloromethane, and PVA is

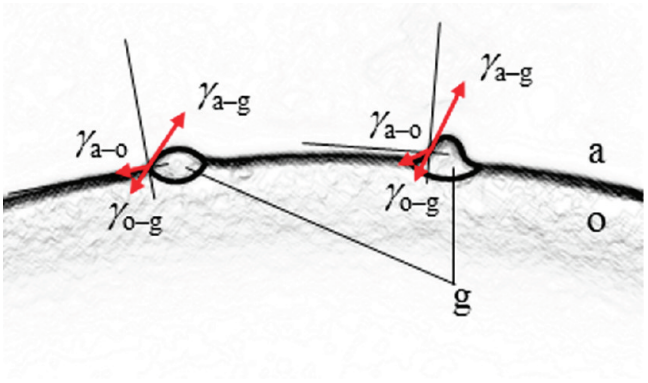

Figure 6. Schematics of the interfacial tensions around the bubbles at the triple phase interface between the aqueous phase (a), organic phase (o), and gas phase (g).

in contact with the mixture of air and dichloromethane gas at the interface between the aqueous phase and gas phase. On the other hand, dichloromethane containing PLA and water is in contact with the mixture of air and dichloromethane gas at the interface between the organic phase and gas phase. Therefore, $\gamma_{w\text{-}air} > \gamma_{a\text{-}g} > \gamma_{o\text{-}g} > \gamma_{d\text{-}air}$. When the top part of a bubble is exposed to the aqueous phase (left schematic in Figure 6), $\gamma_{a\text{-}o}$ is in the tangential direction of a droplet. Because $\gamma_{a\text{-}g} > \gamma_{o\text{-}g}$, the bubble moves toward the aqueous phase. As this occurs, the direction of $\gamma_{a\text{-}o}$ goes downward (right schematic in Figure 6). However, because the dichloromethane concentration decreases in the aqueous phase, $\gamma_{a\text{-}g}$ increases, causing the bubble to still move toward the aqueous phase. To elucidate this release mechanism, it is necessary to predict the interfacial tensions at the triple phase interface by considering the local PLA shell properties.

4.3. Size Control Using the Bubble Template Method. It is noted that even if the release mechanism is single-bubble release as a result of solvent evaporation (Figure 5a), the fabricated hollow PLA microcapsules are smaller than the template microbubbles. Assuming that all of the dichloromethane gas diffuses into the aqueous medium and only air gas remains in the template bubbles, the fabricated hollow PLA microcapsules are still smaller than the template air bubbles. It is possible that the size of the hollow capsules depends on some structural and dynamic properties of the shell materials in addition to the size of template microbubbles. Inside the droplets, the PLA chain configuration is swollen because dichloromethane is a good solvent, while in the surrounding aqueous medium, the PLA chain configuration is globular.[23−25] Therefore, when the microbubbles covered with PLA pass through the interface, the PLA chain configuration changes to form coils. As a result, the possible surface area covered with the PLA coils decreases, yielding smaller hollow PLA microcapsules. Furthermore, if PVA is present in the aqueous medium, it hinders the interactions between PLA and water.[26,27] In particular, the hydrophobic segment of PVA adsorbs onto PLA, which reduces the direct interactions between PLA and water and prevents the PLA capsule shell from shrinking.

In the bubble template method of hollow microcapsules, the bubble dynamics and material properties strongly correlate. In general, the size and uniformity of the capsules depend on bubble dynamics, whereas the shell properties depend on material properties. However, these two cannot be completely separated. In this study, we clarified the factors that affect the size and

uniformity of the fabricated hollow PLA microcapsules and the relationship between the uniformity of the hollow PLA microcapsules and the bubble-release mechanism. However, further investigations of the bubble dynamics at the liquid−liquid interface and the structural and dynamic properties of PLA and PVA are needed to completely understand how the PLA-covered microbubbles are released from the droplets into the surrounding aqueous medium and, as a consequence, how the solidification of the PLA soft shell proceeds.

5. CONCLUSION

To precisely control the size of the hollow PLA microcapsules fabricated using the bubble template method, the effect of the initial PLA concentration, the addition of PVA to the aqueous medium, and PLA molecular weight on the capsule radius distribution were investigated. In addition, the relationship between the uniformity of the hollow PLA microcapsules and the bubble-release mechanism were clarified. The following conclusions were drawn from this study: (1) the initial PLA concentration should be within 2−3 g L^{-1}, which is much lower than the PLA concentration at which the release of bubbles starts, in order to delay release until the dissolving PLA molecules adsorb on the nucleated bubble surface; (2) PVA should be added to the surrounding aqueous medium as a surfactant; and (3) PLA with a low molecular weight should be used. In view of the above three conclusions, the bubble-release mechanism can be classified as either single-bubble release as a result of solvent evaporation or multiple-bubble release as a result of bubble eruption. The first mechanism is required for the fabrication of uniformly sized hollow PLA microcapsules. The bubble-release mechanism remains to be fully elucidated. Further investigations on the bubble dynamics at the liquid−liquid interface and the structural and dynamic properties of PLA and PVA are needed to completely understand the bubble-release mechanism.

■ ASSOCIATED CONTENT

Supporting Information. Figure S1 shows time courses of interfacial tension and droplet volume of either dichloromethane or 2 g L^{-1} PLA (2 kDa) dichloromethane solution measured by the pendant drop method. Figure S2 shows time courses of the droplet volume of either dichloromethane or a 2 g L^{-1} PLA (2 kDa) dichloromethane solution without the addition of liquid in the pendant drop method. In Figures S1 and S2, the surrounding aqueous medium is either water or a 2% (w/w) PVA aqueous solution. Figure S3 shows specific viscosity of the PLA dicholoromethane solutions as a function of the PLA concentration. This material is available free of charge via the Internet at http://pubs.acs.org.

■ AUTHOR INFORMATION

Corresponding Author

*E-mail: daiguji@k.u-tokyo.ac.jp. Phone: +81 4 7136 4658. Fax: +81 4 7136 4659.

■ ACKNOWLEDGMENT

This research was supported by a Grant-in-Aid for Scientific Research (B) (No. 20360093) from the Japan Society for the Promotion of Science (JSPS).

■ REFERENCES

(1) Schutt., E. G.; Klein, D. H.; Mattrey, R. M.; Riess, J. G. *Angew. Chem. Int.* **2003**, *42*, 3218–3235.
(2) Wheatley, M. A.; Schrope, B.; Shen, P. *Biomaterials* **1990**, *11*, 713–717.
(3) Calliada, F.; Campani, R.; Bottinelli, O.; Bozzini, A.; Sommaruga, M. G. *Eur. J. Radiol.* **1998**, *27*, S157–S160.
(4) Ophir, J.; Parker, K. J. *J. Ultrasound Med. Biol.* **1989**, *15*, 319–333.
(5) Lin, P.; Eckersley, R.; Hall, E. *Adv. Mater.* **2009**, *21*, 3949–3952.
(6) Lathia, J. D.; Leodore, L.; Wheatley, M. A. *Ultrasonics* **2004**, *42*, 763–768.
(7) Wheatley, M. A.; Forsberg, F.; Oum, K.; Ro, R.; El-Sherif, D. *Ultrasonics* **2006**, *44*, 360–367.
(8) Ferrara, K.; Pollard, R.; Borden, M. *Annu. Rev. Biomed. Eng.* **2007**, *9*, 415–447.
(9) Plesset, M. S.; Sadhal, S. S. *Appl. Sci. Res.* **1982**, *38*, 133–141.
(10) Kabalnov, A.; Bradley, J.; Flaim, S.; Klein, D.; Pelura, T.; Peters, B.; Otto, S.; Reynolds, J.; Schutt, E.; Weers, J. *Ultrasound Med. Biol.* **1998**, *24*, 751–760.
(11) Leighton, T. G. *The Acoustic Bubble*, 1st ed.; Academic Press: London, 1997.
(12) Shchukin, D. G.; Köhler, K.; Möhwald, H.; Sukhorukov, G. B. *Angew. Chem., Int. Ed.* **2005**, *44*, 3310–3314.
(13) Lin, P.; Eckersley, R.; Hall, E. *Adv. Mater.* **2009**, *21*, 3949–3952.
(14) Narayan, P.; Wheatley, M. A. *Polym. Eng. Sci.* **1999**, *39*, 2242–2252.
(15) Daiguji, H.; Makuta, T.; Kinoshita, H.; Oyabu, T.; Takemura, F. *J. Phys. Chem. B* **2007**, *111*, 8879–8884.
(16) Makuta, T.; Takada, S.; Daiguji, H.; Takemura, F. *Mater. Lett.* **2009**, *63*, 703–705.
(17) Daiguji, H.; Takada, S.; Molino Cornejo, J. J.; Takemura, F. *J. Phys. Chem. B* **2009**, *113*, 15002–15009.
(18) Ward, C. A.; Tikusis, P.; Vender, R. D. *J. Appl. Phys.* **1982**, *53*, 6076–6084.
(19) Boury, F.; Ivanova, Tz.; Panaïotov, I.; Proust, J. E.; Bois, A.; Richou, J. *J. Colloid Interface Sci.* **1995**, *169*, 380–392.
(20) Rubinstein, M.; Colby, R. *Polymer Physics*, 1st ed.; Oxford University Press: Oxford, U.K., 2003.
(21) Shirono, K.; Morimatsu, T.; Takemura, F. *J. Chem. Eng. Data* **2008**, *53*, 1867–1871.
(22) Sugiyama, K; Takemura, F. *J. Fluid Mech.* **2010**, *662*, 209–231.
(23) Athawale, M. V.; Goel, G.; Ghosh, T.; Truskett, T. M.; Garde, S. *Proc. Natl. Acad. Sci. U.S.A.* **2007**, *104*, 733–738.
(24) Jamadagni, S. N.; Godawat, R.; Dordick, J. S.; Garde, S. *J. Phys. Chem. B* **2009**, *113*, 4093–4101.
(25) ten Wolde, P. R.; Chandler, D. *Proc. Natl. Acad. Sci. U.S.A.* **2002**, *99*, 6539–6543.
(26) Kozlov, M.; Quarmyne, M.; Chen, W.; McCarthy, T. J. *Macromolecules* **2003**, *36*, 6054–6059.
(27) Kozlov, M.; McCarthy, T. J. *Langmuir* **2004**, *20*, 9170–9176.